Investigation of cloud-aerosol interaction for extreme precipitation events using NCEP global models

Sheng-Po Chen, Cheng-Hsuan (Sarah) Lu
University at Albany, State University of New York (SUNYA)

Yu-Tai Hou, Anning Cheng, Moorthi Shrinivas, Fanglin Yang
NOAA/National Centers for Environmental Prediction (NCEP)

Arlindo da Silva, Donfian Barahona, Anton Darmenov
NASA/Global Modeling and Assimilation Office (GMAO)

Abstract

While understanding the climate impacts of the complex cloud-aerosol-radiation interactions remains a major frontier in climate sciences, there have been significant processes in developing process-level representations of clouds and aerosols as well as in understanding the processes relevant to aerosol-cloud-radiation interactions. NASA Global Modeling and Assimilation Office (GMAO) is revamping the existing treatments of clouds and aerosols in Goddard Earth Observing System Model, Version 5 (GEOS-5) by introducing a double-moment cloud microphysics scheme and coupling it with a modal aerosol model. The physically-based cloud/aerosol package at GMAO is later implemented into NOAA Global Forecast System (GFS). In this study, GFS is used to simulate two extreme precipitation events: New York snow storm in January 2014 and Louisiana flooding in August 2016. The comparison could provide an insight on optimal configuration for NWP models in the contexts of representing aerosol process. We will also investigate aerosol-cloud microphysics-precipitation interaction and the uncertainty in model precipitation simulation under different climate regimes.

Key word: cloud-aerosol interaction, global forecast system, extreme precipitation event

1. Introduction

The Global Forecast System, dotted as GFS, is the cornerstone of NCEP's operational production suite of numerical guidance. It provides deterministic and probabilistic guidance out to 16 days over a global domain, four times daily at 00, 06, 12, and 18 UTC. In addition, the GFS provides atmospheric initial and/or boundary conditions for other NCEP's models, including regional, hurricane, ocean and wave, and aerosol prediction systems. The atmospheric forecast model used in the GFS is a global spectral model (GSM) with a comprehensive physics suite (the GFS webpage: http://www.emc.ncep.noaa.gov/GFS/doc.php). Here we describe only those parameterizations relevant to our proposed work.

Radiation

The longwave (LW) and the shortwave (SW) radiation parameterizations are modified and optimized versions of the Rapid Radiative Transfer Models for general circulation models (GCM) (i.e., RRTMG_LW v2.3 and RRTMG_SW v2.3, respectively) developed at Atmospheric & Environmental Research (AER) Inc. *[Clough et al., 2005; Iacono et al., 2000; Mlawer et al., 1997]*. The LW algorithm contains 140 unevenly distributed g-points in 16 broad spectral bands, while the SW algorithm includes 112 g-points in 14 bands. In addition to the major atmospheric absorbing gases of ozone, water vapor, and carbon dioxide, the algorithm also considers various minor absorbing species such as methane, nitrous oxide, oxygen, and up to four types of halocarbons (CFCs). Concentrations of atmospheric greenhouse gases are either obtained from global network measurements, such as carbon dioxide (CO_2), or taking the climatological constants, such as methane, nitrous oxide, oxygen, and CFCs. A maximum-random cloud overlapping method is used in both LW and SW calculations. Cloud condensate path and effective radius for water and ice are used for the calculation of cloud-radiative properties. Hu and Stamnes' method *[Hu and Stamnes, 1993]* is used to treat water clouds in both LW and SW parameterizations. For ice clouds, Ebert and Curry's method *[Ebert and Curry, 1992]* is used for the LW while Fu's scheme *[Fu, 1996]* is used for the SW.

A tropospheric climatological aerosol distribution at 5-degree resolution *[Hess et al., 1998]* is used in both

LW and SW radiations. A generalized spectral mapping scheme was developed to compute aerosol optical properties at each radiation spectral band. A separate stratospheric volcanic aerosol scheme was added that is capable of handling volcanic eruption events. In SW, incoming solar constant is held constant at 1366 W/m^2 in the operational GFS. An option to use an eleven-year solar cycle was added for long term simulation (or climate) purpose. The SW albedo scheme uses surface vegetation type based seasonal climatology similar to that described Hou et al. *[Hou et al., 2002]* but with a modification in the treatment of solar zenith angle dependency over snow-free land surface *[Yang et al., 2008]*. Black-body surface emissivity is assumed for the LW radiation. In the operational GFS, the CO_2 value is estimated from the most recent five-year observations.

Cloud fraction and cloud microphysics

For the calculations of radiative fluxes, the fractional area of the grid box covered by the clouds is computed diagnostically from the relative humidity, condensate mixing ratio, and saturation mixing ratio following Xu and Randall *[Xu and Randall, 1996]*. The grid-scale condensation is based on the cloud microphysics parameterization of Zhao and Carr *[Zhao and Carr, 1997]*, which in turn is based on Sundqvist et al. *[Sundqvist et al., 1989]*. The sinks of the cloud condensate include grid-scale precipitation, parameterized following Zhao and Carr *[Zhao and Carr, 1997]* for ice water, Sundqvist et al. *[Sundqvist et al., 1989]* for liquid water, and evaporation of the cloud condensate, parameterized following Zhao and Carr *[Zhao and Carr, 1997]*. Evaporation of rain in the unsaturated layers below the level of condensation is taken into account. In general, tropical clouds are primarily due to convective anvils resulting from cumulus detrainment, while extratropical clouds arise mainly through grid-scale condensation.

Cloud fraction in the microphysics scheme is diagnosed as a function of relative humidity alone following Sundqvist et al. *[Sundqvist et al., 1989]*. Three values of critical humidity may be specified (near the surface, at the top of the boundary layer and at the model top with interpolated values in between) though only a single value is currently used. While this value can be specified externally, it is assumed that it is applicable at the equator at T62 resolution and the critical relative humidity at any grid point is calculated through interpolation between this specified value and 100% relative humidity corresponding to very high resolution. The Ferrier scheme, a double-moment bulk cloud microphysics scheme used in the NCEP North American Mesoscale Model (NAM) *[Ferrier et al., 2002]*, is an option in the GFS physics suite.

2. Model configuration

The cloud microphysics scheme in GEOS-5 is a double-moment cloud microphysics scheme (i.e., MG scheme) considering the evolution of ice and liquid mass mixing ratio and number concentration *[Barahona et al., 2014; Gettelman et al., 2008; Morrison and Gettelman, 2008]*. It explicitly treats processes of condensation, evaporation, collection, melting, freezing, and sedimentation (**Fig. 1**). Cloud droplet and ice crystal production rates are computed considering the aerosol properties, temperature, and the subgrid-scale dynamics. Cloud droplet activation is computed linking explicitly to the aerosol composition and size distribution *[Fountoukis and Nenes, 2005]*. Similarly, ice crystal nucleation is treated using a physically-based analytical approach *[Barahona and Nenes, 2009]*. Homogeneous freezing of cloud droplets and haze particles as well as heterogeneous freezing of ice nuclei in the immersion, and contact modes are accounted for.

The upgrade in how cloud microphysical processes are represented in NOAA Environmental Modeling System (NEMS) GSM lead to additional development work (**Fig. 2**). For instance, the MG scheme has been coupled with PDF-based cloud scheme (Simplified Higher-Order Closure, SHOC) and convective parameterization (Relaxed Arakawa Schubert, RAS, *[Moorthi and Suarez, 1992]*). The MG development work has been using similar parameters diagnosed from the bulk Goddard Chemistry Aerosol Radiation and Transport (GOCART) scheme. Note the MG implementation has been accelerated by the National Weather Service (NWS) internal Research-to-Operation (R2O) project led by Dr. Shrinivas Moorthi. Extensive code development for bringing in MG into NEMS GSM and coupling MG with other physics in NEMS GFS physics suite are made by Dr. Moorthi's team while this study has been focused on coupling of the aerosol physicochemical properties to cloud formation through cloud condensation nuclei (CCN) and ice nuclei (IN) activation and investigating aerosol-cloud interaction through a series of NEMS GSM experiments.

The NEMS GSM experiments are conducted for selected cases, including 2014 New York snow storm, 2016 Louisiana flooding and 2016 Hurricane Matthew. Here we present the results for the 2016 Louisiana flooding case. T574 L64 NEMS GSM experiments are conducted for the Aug 8–17, 2016 period. The NEMS GSM configuration is same as the operational NEMS GFS Aerosol Component (NGAC) version 2 (NEMS GSM with prognostics GOCART turned on) except dynamics is changed from Eulerian to semi-Lagrangian and resolution is increased from T126 (~100 km) to T574 (~35 km). Initial conditions for these experiments are taken from operational Global Data Assimilation System at T1534 (~13 km) except for aerosol fields which are determined from NGACv2 at T126. Three scenarios are considered: (1) the control (CTRL) run with Zhao-Carr cloud microphysics without aerosol activation, (2) the MG_NoAER run with MG cloud microphysics without aerosol activation, and (3) the MG_AER (or MG_GOCART) run with MG cloud microphysics with aerosol activation by GOCART. Note the aerosol attenuation in RRTMG radiation module *[Clough et al., 2005; Iacono et al., 2000; Mlawer et al.,* *1997]* is determined from the OPAC climatology based on Hess et al. *[Hess et al., 1998]* (the operational configuration), allowing this study to focus on aerosol-cloud interaction.

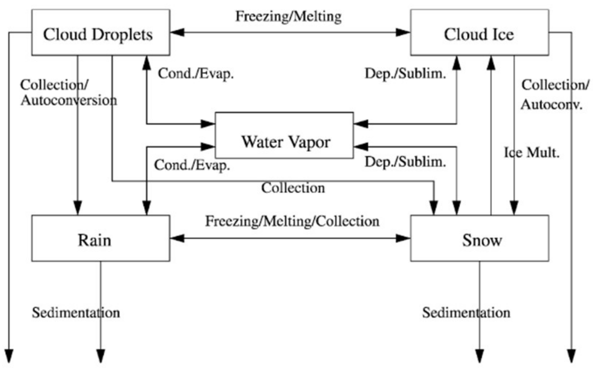

Fig. 1. Processes represented in MG cloud microphysics scheme.

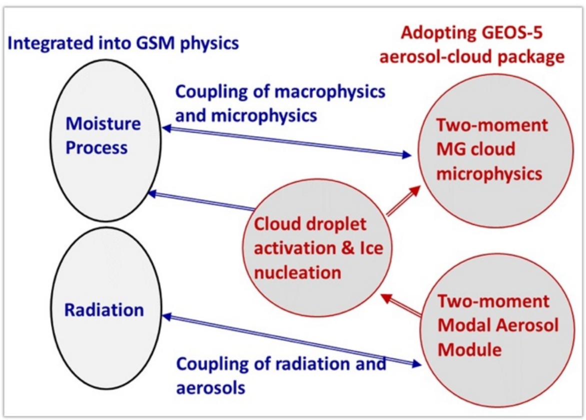

Fig. 2. The coupling between GEOS-5 aerosol-cloud package and NEMS GFS physics suite.

3. Results and discussion

Fig. 3 shows the global-averaged daily-mean cloud fraction from the three NEMS GSM runs, compared with reanalysis from several datasets, including NASA MERRA2 (the Modern-Era Retrospective analysis for Research and Applications, Version 2) and satellite-derived cloud products from PATMOS-x (Pathfinder Atmospheres–Extended), MODIS (Moderate Resolution Imaging Spectroradiometer), and CERES (Clouds and the Earth's Radiant Energy System). Overall, the cloud fraction from the three NEMS GSM experiments shows low biases compared to MERRA2 reanalysis and satellite estimates. The low bias in cloud fraction is improved as the model physics suite is upgraded to the MG scheme. Previous studies comparing GFS (GSM without NEMS framework) with International Satellite Cloud Climatology Project (ISCCP) also show global underestimation in total cloud cover.

Zonal averaged cloud fraction as a function of latitude from NEMS GSM runs, MERRA2, and satellite products is shown in **Fig. 4**. Overall NEMS GSM has better agreement with observations and reanalysis in north tropical region (the equator to 30N). The CTRL run has consistently lower cloud cover than other two NEMS GSM runs with MG scheme. The largest discrepancy is found around north-hemisphere mid-latitude area and south-hemisphere polar region. The MG_AER run shows better agreement with MERRA2 and satellite observations. The results presented here (higher cloud fraction in MG results than CTRL but still lower than satellite retrievals) are consistent with GEOS-5 results presented in Barahona et al. *[Barahona et al., 2014]*.

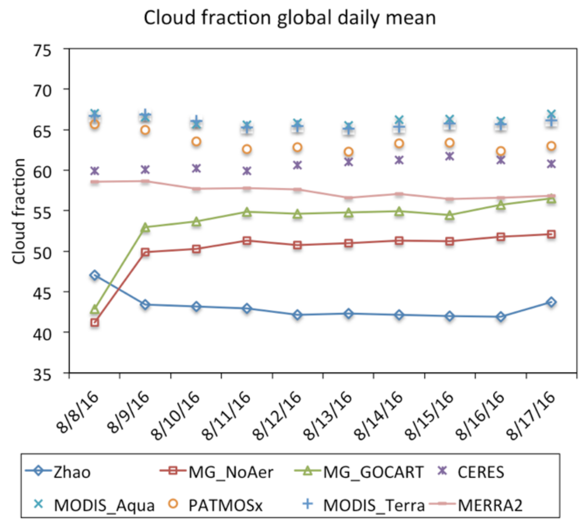

Fig. 3. Global daily mean cloud fraction from NEMS GSM experiments, MERRA2, and satellite products for Aug 8-17, 2016.

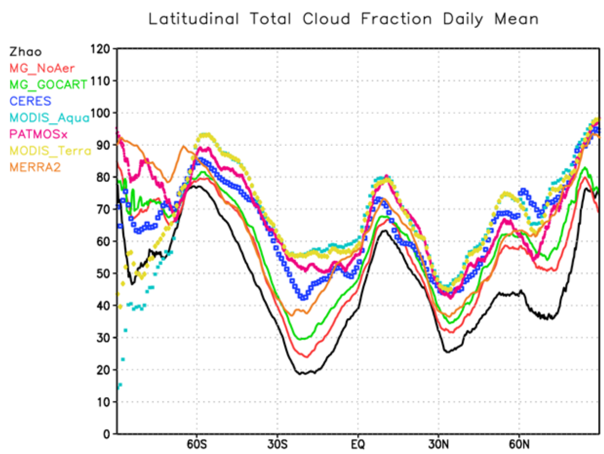

Fig. 4. Zonal averaged cloud cover from NEMS GSM, MERRA2, and satellite retrievals.

Fig. 5 shows high-level cloud optical depth from three NEMS GSM runs averaged for the Aug 10-17, 2016 period, compared with CERES estimates. All three model runs have lower high-level cloud optical depth compared with the CERES estimates. The CTRL run has the lowest cloud optical depth. The MG_NoAER and MG_AER runs have similar spatial pattern, suggesting the improvement in cloud optical depth is mainly resulted from the change in cloud microphysics scheme, not in aerosol activation.

Latitude-height cross section of zonal mean liquid and ice cloud mas mixing ratios is displayed in **Fig. 6**. While the Zhao-Carr scheme only has mixed-phase cloud condensate, the MG scheme considers ice and liquid separately. Both MG_NoAER and MG_AER show similar latitudinal variations, especially for liquid cloud. At high altitudes MG_NoAER has lower [higher] ice cloud mass mixing ratios than MG_AER in the tropical region [mid-latitude region]. When compared with MERRA2, MG_AER has better agreement than MG_NoAER in the tropical region. Too much tropical high cloud is produced in the CTRL run. This feature is not found in MG runs and MERRA2.

Despite the improvement in cloud properties by adopting the MG scheme, the impact of physics upgrade on precipitation is insignificant for this case. **Fig. 7** shows the daily precipitation for Aug 13 2016 from the three NEMS GSM runs compared with Climate Prediction Center (CPC) rain gauge observations. Overall, the model predicted precipitation is low compared with rain gauge and rain band observed at Texas and Oklahoma is not captured by the model regardless of physics configuration.

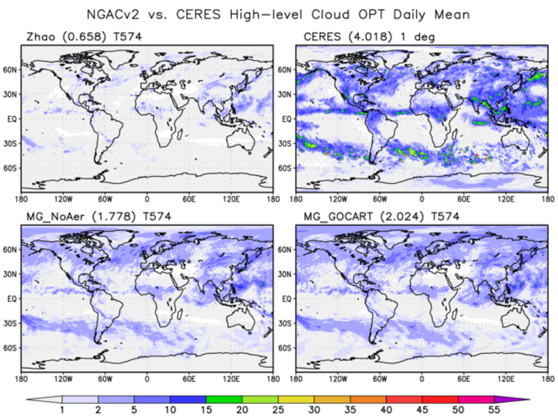

Fig. 5. High-level cloud optical depth from NEMS GSM runs and CERES estimates, averaged for Aug 10-17, 2016.

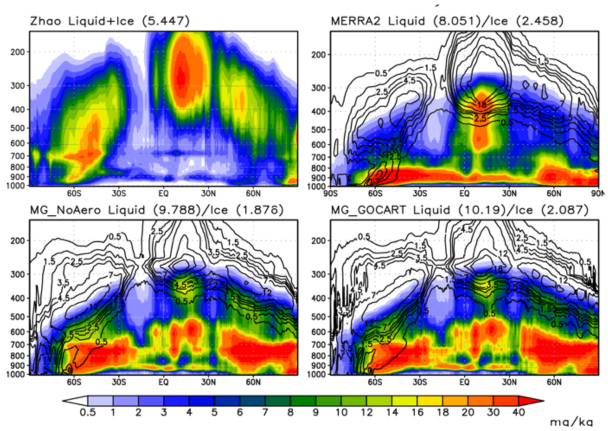

Fig. 6. Cross section of zonal mean liquid and ice cloud mass mixing ratios for NEMS GSM runs and MERRA2.

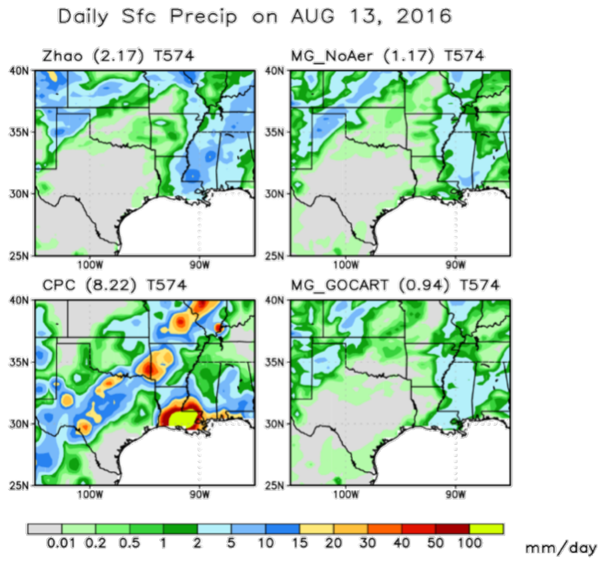

Fig. 7. Daily precipitation for CTRL, MG_NoAER, MG_AER runs, compared with CPC rain gauge observations for Aug 13, 2016.

4. Summary

The new implementation for cloud microphysics resulted in a general model improvement in cloud properties for NEMS GFS. Cloud droplet and ice crystal number concentrations are now available as prognostic fields. Also, the new cloud microphysics is allowed for aerosol activation. However, better cloud fields do not necessary lead to better weather prediction. Some tuning and adjustments will be needed in future. The need for model refinement in turn calls for the need to enhance the model evaluation and verification package. The traditional GFS verification package is not sufficient to evaluate these physically-based schemes. For instance, cloud related diagnostics was not outputted in the operational GFS and has been added to NEMS GSM. Observation-based diagnosis package is needed to examine whether the model with improved aerosol-cloud package better capture the aerosol/cloud properties and the processes relevant to aerosol-cloud-radiation interaction.

References

Barahona, D., A. Molod, J. Bacmeister, A. Nenes, A. Gettelman, H. Morrison, V. Phillips, and A. Eichmann (2014), Development of two-moment cloud microphysics for liquid and ice within the NASA Goddard Earth Observing System Model (GEOS-5), *Geosci. Model Dev.*, *7*(4), 1733-1766, doi:10.5194/gmd-7-1733-2014.

Barahona, D., and A. Nenes (2009), Parameterizing the competition between homogeneous and heterogeneous freezing in ice cloud formation – polydisperse ice nuclei, *Atmos. Chem. Phys.*, *9*(16), 5933-5948, doi:10.5194/acp-9-5933-2009.

Clough, S. A., M. W. Shephard, E. J. Mlawer, J. S. Delamere, M. J. Iacono, K. Cady-Pereira, S. Boukabara, and P. D. Brown (2005), Atmospheric radiative transfer modeling: a summary of the AER codes, *Journal of Quantitative Spectroscopy and Radiative Transfer*, *91*(2), 233-244, doi:https://doi.org/10.1016/j.jqsrt.2004.05.058.

Ebert, E. E., and J. A. Curry (1992), A parameterization of ice cloud optical properties for climate models, *97*(D4), 3831-3836, doi:10.1029/91jd02472.

Ferrier, B. S., Y. Jin, Y. Lin, T. Black, E. Rogers, and G. Dimego (2002), *Implementation of a new grid-scale cloud and precipitation scheme in the NCEP Eta model*, 280-283 pp.

Fountoukis, C., and A. Nenes (2005), Continued development of a cloud droplet formation parameterization for global climate models, *110*(D11), doi:10.1029/2004jd005591.

Fu, Q. (1996), An Accurate Parameterization of the Solar Radiative Properties of Cirrus Clouds for Climate Models, *9*(9), 2058-2082, doi:10.1175/1520-0442(1996)009<2058:Aapots>2.0.Co;2.

Gettelman, A., H. Morrison, and S. J. Ghan (2008), A New Two-Moment Bulk Stratiform Cloud Microphysics Scheme in the Community Atmosphere Model, Version 3 (CAM3). Part II: Single-Column and Global Results, *21*(15), 3660-3679, doi:10.1175/2008jcli2116.1.

Hess, M., P. Koepke, and I. Schult (1998), Optical Properties of Aerosols and Clouds: The Software Package OPAC, *79*(5), 831-844, doi:10.1175/1520-0477(1998)079<0831:Opoaac>2.0.Co;2.

Hou, Y. T., S. Moorthi, and K. A. Campana (2002), Parameterization of solar radiation transfer in the NCEP models*Rep.*, 46 pp, NCEP Office Note 441.

Hu, Y. X., and K. Stamnes (1993), An Accurate Parameterization of the Radiative Properties of Water Clouds Suitable for Use in Climate Models, *6*(4), 728-742, doi:10.1175/1520-0442(1993)006<0728:Aapotr>2.0.Co;2.

Iacono, M. J., E. J. Mlawer, S. A. Clough, and J.-J. Morcrette (2000), Impact of an improved longwave radiation model, RRTM, on the energy budget and thermodynamic properties of the NCAR community climate model, CCM3, *105*(D11), 14873-14890, doi:10.1029/2000jd900091.

Mlawer, E. J., S. J. Taubman, P. D. Brown, M. J. Iacono, and S. A. Clough (1997), Radiative transfer for inhomogeneous atmospheres: RRTM, a validated correlated-k model for the longwave, *102*(D14), 16663-16682, doi:10.1029/97jd00237.

Moorthi, S., and M. J. Suarez (1992), Relaxed Arakawa-Schubert. A Parameterization of Moist Convection for General Circulation Models, *120*(6), 978-1002, doi:10.1175/1520-0493(1992)120<0978:Rasapo>2.0.Co;2.

Morrison, H., and A. Gettelman (2008), A New Two-Moment Bulk Stratiform Cloud Microphysics Scheme in the Community Atmosphere Model, Version 3 (CAM3). Part I: Description and Numerical Tests, *21*(15), 3642-3659, doi:10.1175/2008jcli2105.1.

Sundqvist, H., E. Berge, and J. E. Kristjánsson (1989), Condensation and Cloud Parameterization Studies with a Mesoscale Numerical Weather Prediction Model, *117*(8), 1641-1657, doi:10.1175/1520-0493(1989)117<1641:Cacpsw>2.0.Co;2.

Xu, K.-M., and D. A. Randall (1996), A Semiempirical Cloudiness Parameterization for Use in Climate Models, *53*(21), 3084-3102, doi:10.1175/1520-0469(1996)053<3084:Ascpfu>2.0.Co;2.

Yang, F., K. Mitchell, Y.-T. Hou, Y. Dai, X. Zeng, Z. Wang, and X.-Z. Liang (2008), Dependence of Land Surface Albedo on Solar Zenith Angle: Observations and Model Parameterization, *47*(11), 2963-2982, doi:10.1175/2008jamc1843.1.

Zhao, Q., and F. H. Carr (1997), A Prognostic Cloud Scheme for Operational NWP Models, *125*(8), 1931-1953, doi:10.1175/1520-0493(1997)125<1931:Apcsfo>2.0.Co;2.